Spectroscopy of image-potential states with inverse photoemission

D. Straub and F. J. Himpsel
IBM Thomas J. Watson Research Center, Yorktown Heights, New York 10598
(Received 16 August 1985)

The binding energies of image-potential states are studied in a systematic way for metals [Cu(111), Cu(100), Cu(110), Ag(111), Au(111), and Au(100)], a semimetal [Sb(100)], and a layered compound ($1T$-TiS_2). Data for Au(111) show that image-potential states exist even in the presence of bulk states. The coupling with bulk states is weak as indicated by the narrow (≤ 0.1 eV) width of the image states. The binding energies of the lowest state cluster around 0.7 eV for a variety of metal and semimetal surfaces indicating a universal phenomenon. This value is close to the hydrogenic binding energy of $\frac{1}{16}$ Ry ~ 0.85 eV for the $n=1$ state, which indicates that the simple Coulombic image potential dominates the energy balance.

I. PERSPECTIVE

Two-dimensional electronic states have received much attention in recent years. Surface states[1] in the gap of bulk energy bands have been found for nearly every clean single-crystal surface. They are sensitive to the potential in the vicinity of the outermost layer. Even in the case where surface and bulk states are energetically degenerate and hybridize with each other one has been able to observe surface resonances,[2] i.e., electronic states with high amplitude near the surface. Another major field of research concerns the two-dimensional electron gas at semiconductor interfaces which exhibits novel transport properties[3] including the quantum Hall effect. Electrons can also be trapped at the surface of liquid helium[4] by their own image force and exhibit interesting phase transitions. The image potential is quite simple compared with the complex potential at the outermost layer of a solid or with the effective potential for an electron gas in a semiconductor.[3] A purely Coulombic image force (compare Fig. 1) gives rise to a hydrogenic series[2,4] of bound energy levels

$$E_n = -[(\tfrac{1}{16}\,\mathrm{Ry}) \times Z_{\mathrm{eff}}^2]/n^2 \quad (1)$$

converging towards the vacuum level ($E=0$). For finite momentum parallel to the surface, $k_{||}$, one has to add the kinetic energy term $(\hbar k_{||})^2/2m^*$ to Eq. (1) where deviations from a simple free-electron behavior can be accommodated by an effective mass m^*. The connection between image potential states and the hydrogen atom can be seen by comparing the kinetic energy terms in the corresponding one-dimensional and three-dimensional Schrödinger equations. The kinetic energy perpendicular to the surface $(d^2/dz^2)\psi_{\mathrm{image}}(z)$ corresponds to $\Delta\psi_{\mathrm{hydrogen}} = (1/r)(\partial^2/\partial r^2)(r\psi_{\mathrm{hydrogen}}) + (\text{angular terms})$. Thus, the Schrödinger equation for the image-potential state is equivalent to the radial equation for an s state of the hydrogen atom with $\psi_{\mathrm{image}}(z) \propto z\psi_{\mathrm{hydrogen}}(z/4)$. The binding energy of the $n=1$ image potential state is 16 times smaller than the Rydberg constant of the hydrogen atom because of an extra factor $\frac{1}{4}$ in the Coulomb energy term. The effective image charge Z_{eff} is close to unity for metal surfaces, but generally it depends on the dielectric constant ϵ of the solid:

$$Z_{\mathrm{eff}} = (\epsilon - 1)/(\epsilon + 1)\,. \quad (2)$$

It becomes significantly smaller than unity for typical semiconductors ($Z_{\mathrm{eff}}^2 = 0.7$ for Si) and can reach very small values[4] for insulators like He ($Z_{\mathrm{eff}}^2 \simeq 8\times 10^{-4}$). Consequently, one expects the largest binding energy of 0.85 eV ($=\frac{1}{16}$ Ry) for metal surfaces. The maximum of the squared $n=1$ wave function lies four Bohr radii outside the image plane ($z=z_0$ in Fig. 1). The reference plane for the image charge is a certain distance x_0 outside[5] the "jellium edge" which is half an interplanar spacing outside the last atomic plane. Typically these values add up to a distance of about 4 Å outside the last lattice plane for the $n=1$ wave function. At this distance the perturbation of the image potential state due to the outer-

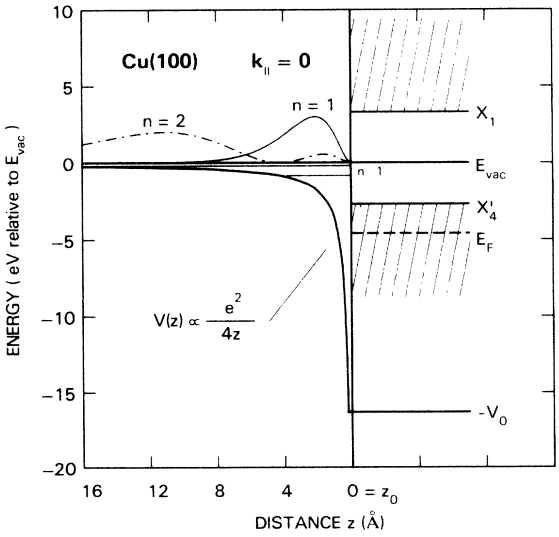

FIG. 1. Model potential diagram for image-potential surface states on Cu(100).

most atomic layer might be small enough to preserve the simple picture of a Rydberg series with only small adjustments in the binding energy. This would make the appearance of image-potential states at metal surfaces a ubiquitous phenomenon which does not depend on the particular material chosen. One of the goals of this work is to test the viability of this thesis.

Image-potential states have been predicted for a fairly long time[4,6–8] but could not be observed directly by conventional surface probes such as photoemission and electron scattering because the electrons are bound and cannot leave the surface.[9] Inverse photoemission (or bremsstrahlung spectroscopy in the ultraviolet) is the ideal technique for probing bound states by observing radiative transitions from continuum states into bound states (for reviews see Ref. 10). Several observations of image potential states were made using this technique.[11–31] We were able to resolve a single member of the Rydberg series[14] using the best energy resolution [$\Delta E = 0.3$ eV (Ref. 32)] achieved in inverse photoemission so far. Recently, image-potential states were seen as intermediate states in two-photon photoemission.[33,34] They also play a role in scanning tunneling microscopy.[35,36]

In this paper we report inverse photoemission data for a wide variety of materials and surfaces, i.e., low-index crystallographic planes of Cu, Ag, Au, Sb, and $1T$-TiS_2. Thereby, various trends in the binding energy of the image-potential states are studied. The material is varied while keeping the position of the bulk band gap relative to the vacuum level roughly the same by choosing the same crystallographic orientation (Sec. III). We also vary the position of the band gap by changing the crystallographic orientation (see Fig. 2 and Sec. IV). This case is particularly interesting because for Au(111) the image-potential state does not fall into a bulk band gap.[37] Therefore, the electron is not Bragg-reflected by the crystal and can escape from the image-potential state into the bulk. By changing the crystallographic orientation we also change the corrugation of the surface and are able to estimate the influence of the crystal potential on the binding energy of the image-potential states (Sec. V). A possible correlation between the effective mass of the image-potential states and their binding energies is considered (Sec. VI) and the predictions of various theoretical models are tested (Sec. VII).

II. INVERSE PHOTOEMISSION EXPERIMENT

Figures 3–7 show angle-resolved inverse photoemission spectra for a variety of surfaces. The spectral distribution of the emitted photons is given for a fixed energy of the incident electron E_i. The cutoff at high photon energies (left-hand side of the spectra) corresponds to final states at the Fermi level E_F. The light was collected at about 45° from the sample normal with equal detection efficiency for both polarization directions. The electrons were incident normal to the sample surface, i.e., the momentum parallel to the surface $k_{||} = 0$.

The metal samples were prepared in a separate preparation chamber by multiple cycles of ion bombardment and mild annealing. Sb(100) and $1T$-TiS_2 were prepared by cleaving the sample *in vacuo*. The pressure in the preparation chamber was better than 2×10^{-10} torr. The samples were then transferred under vacuum into the

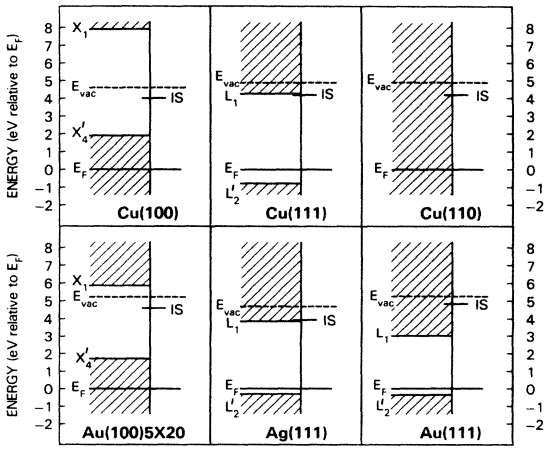

FIG. 2. Positions of bulk band gaps and image-potential surface states for the measured Cu, Au, and Ag-surfaces at $k_{||} = 0$.

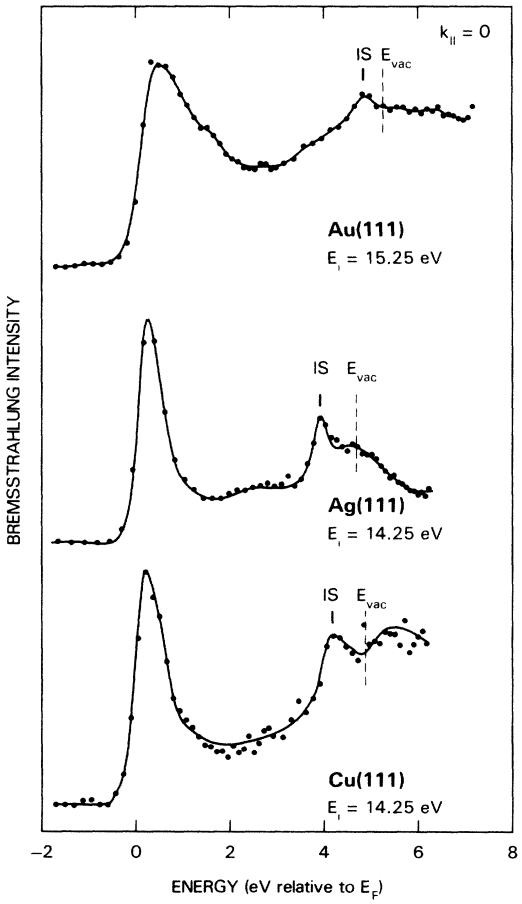

FIG. 3. Inverse photoemission spectra for Au(111), Ag(111), and Cu(111) for normal electron incidence.

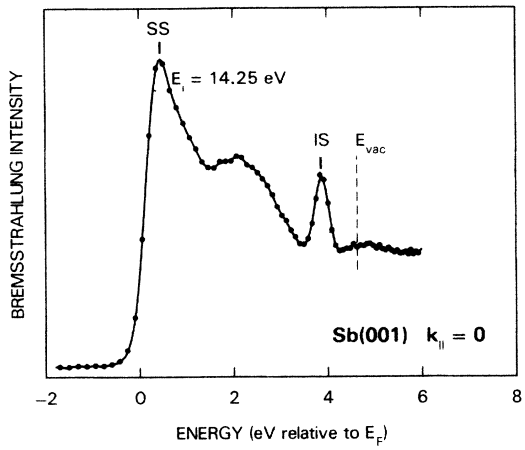

FIG. 4. Inverse photoemission spectrum for Sb(100). This surface exhibits the $n=1$ image-potential state at 3.93 eV and a crystal-induced surface state at the Fermi level.

measurement chamber with a base pressure of better than 5×10^{-11} torr during data collection.

The binding energy of the image-potential states is referred to the vacuum level E_{vac} whereas the inverse photoemission measurement gives energies with respect to the Fermi level. Thus, an exact knowledge of the work function Φ of the actual sample surface is essential for an exact determination of the image-potential-state binding

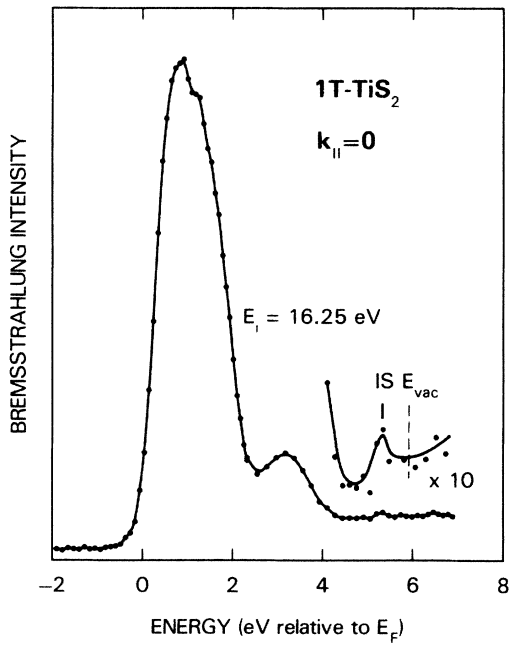

FIG. 5. Inverse photoemission spectrum for 1T-TiS_2. The spectrum was taken for electron incidence normal to the basal plane. Note that the intensity of the image potential state is scaled down relative to the strong d band emission at about 1.5 eV. The absolute intensity of the $n=1$ image state is comparable to the intensity obtained from noble metals which have no unoccupied d states.

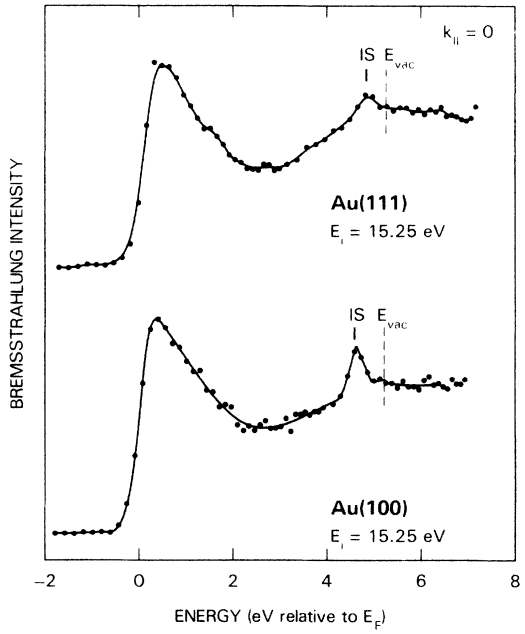

FIG. 6. Inverse photoemission spectra for Au(111) and Au(100) for normal electron incidence.

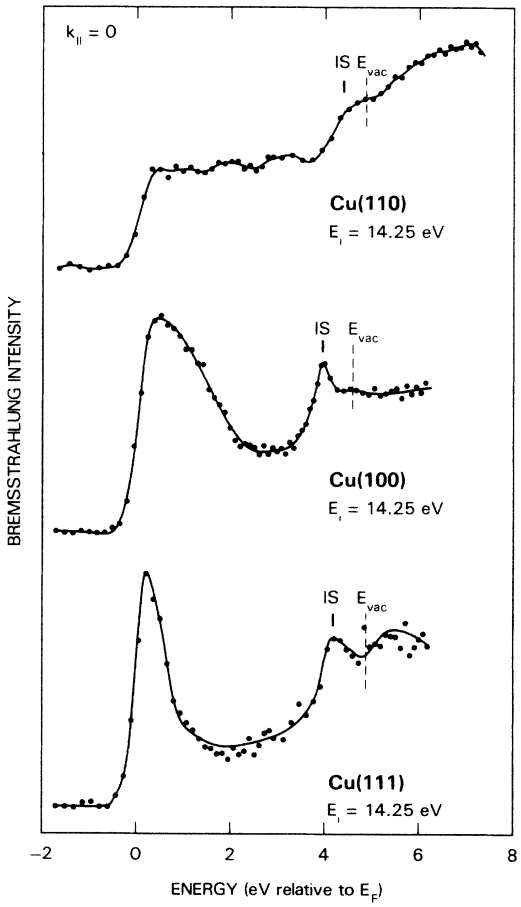

FIG. 7. Inverse photoemission spectra for Cu(111), Cu(100), and Cu(110) for normal electron incidence.

energy. Therefore, we measured the work function *in situ* using a piezoelectrically driven Kelvin probe[38] for the Ag(111), Cu(111), Cu(110), Sb(100), and TiS_2 surfaces. The work function of the probe was calibrated against cleaved Si(111) surfaces which have a very reproducible work function of 4.85 eV almost independent of doping and cleavage quality.[39,40]

III. MATERIALS

In going from Ag(111) to Cu(111) to Au(111) we keep the surface structure the same but increase in the position of the vacuum level E_{vac} from 4.69 to 4.88 to 5.26 eV (Ref. 41) above E_F (dashed line in Fig. 3). The image-potential state at about 0.7 eV below the vacuum level follows this jump in the vacuum level thereby keeping its binding energy nearly constant. The largest deviation from this value is found for Au(111) where the binding energy is 0.1—0.2 eV lower. In order to see whether or not this universality carries further, we have tested dissimilar materials, namely, the semimetal antimony and a layered compound, the transition-metal dichalcogenide TiS_2. As shown in Figs. 4 and 5 there exist image-potential states again and with a binding energy of 0.76 eV on Sb (Ref. 23) and 0.60 eV on TiS_2 (Ref. 24) similar to that for noble metals. A surface state previously observed on graphite[42] is another possible candidate for an image-potential state on a semimetal. A complete tabulation of existing data measured by several groups for vari-

TABLE I. Summary of available data on binding energies E_B and effective masses m^* for image-potential surface states. The work functions Φ are taken from the references given with the reported binding energies.

Sample	Φ (eV)	Ref.	E_B (eV)	m^*/m_e	Ref.
Au(100)	5.22	43	0.63		14
Au(110)			observed, no value given		35
Au(111)	5.26	41	0.42±0.16		this work
Ag(100)	4.6	46	0.5±0.2	1.2±0.2	26,28
Ag(100)			0.5	1.6±0.3	16
Ag(100)[a]	4.42	34	0.53±0.03 ($n=1$)	1.15±0.15	34
			0.16±0.03 ($n=2$)		34
Ag(110)			observed, no value given		35
Ag(111)	4.74	46	0.9	1.0	25
Ag(111)[a]	4.69	this work	0.77±0.10		this work
Ag(111)	4.74	46	0.6±0.2	1.4±0.3	26,28
Ag(111)	4.74	46	0.65	1.3±0.3	45
Ag(111)[a]	4.56	34	0.77±0.03 ($n=1$)	1.35±0.15	33,34
			0.23±0.03 ($n=2$)		33,34
Cu(100)			observed, no value given		11
Cu(100)	4.59	47	0.6±0.2	1.2±0.2	12
Cu(100)	4.5	48	0.8	1.2±0.2	13
Cu(100)	4.59	48	0.64		14
Cu(100)			0.62	0.98	31
Cu(100)[a]	4.60	34	0.57±0.03 ($n=1$)	0.9±0.1	34
			0.18±0.03 ($n=2$)		34
Cu(110)[a]	4.87	this work	0.48±0.15		this work
Cu(110)			observed, no value given		21
Cu(111)[a]	4.88	this work	0.70±0.15		this work
Cu(111)	4.88	33,34	0.83±0.03		33,34
Cu(111)	4.94	49	0.94±0.15	1	19
Cu(111)	4.98	47	0.8±0.2	1.2±0.2	26,27
Ni(100)	5.2	50	0.4±0.2	1.2±0.2	22
Ni(100)	5.2		observed, no value given		11
Ni(110)	5.04	52	0.6±0.2	1.7±0.3	20[b]
Ni(111)	5.2	51	0.6±0.2	1.6±0.2	22
Ni(111)[a]	5.25	33,34	0.80±0.03		33,34
Pd(111)			observed, no value given		15
Pd(111)	5.55	53	0.85		29
Pt(111)	5.93	54	0.63		26
Fe(110)	5.1	55	0.4		30
Sb(100)[a]	4.69	23	0.76±0.10		23
1*T*-TiS_2[a]	5.92	this work	0.60±0.10		this work

[a]Work-function measurements for these samples were taken *in situ*.

[b]The reported value was obtained by extrapolation to $k_{||}=0$.

ous materials is undertaken in Table I. We attempted to go on to an even wider class of materials such as semiconductors (Si,Ge,GaAs) which have dielectric constants low enough to expect a significant ($\sim 30\%$) reduction in binding energy due to the reduced image charge. In our initial studies we have found no obvious candidates for image-potential states on semiconductors. The large and very structured density of bulk states near the vacuum level may prevent us from seeing them.

IV. HYBRIDIZATION WITH BULK STATES

The reconstruction of the Au(100)5×20 surface allows us to compare with the Au(111)1×1 surface which has virtually the same surface potential but a different position of the bulk band gap (Figs. 2 and 6). The reconstructed Au(100)5×20 surface has a close-packed Au(111) plane at the surface which is somewhat rippled to come into near registry with the substrate (see Ref. 56 and references therein). For the Au(100)5×20 surface the image-potential state lies within a bulk band gap at $k_{||}=0$; for Au(111)1×1 it overlaps bulk bands. It is apparent from Fig. 6 that the image-potential state still exists for Au(111)1×1 but is weakened by about a factor of 2 compared with the other surface. This could be due to the formation of a surface resonance via hybridization with the underlying bulk states. From the amount of attenuation one should be able to deduce the strength of the coupling between image states and bulk states. Another measure of the coupling is the width of the image state. Using the derivative of the observed cutoff function at the Fermi level as our resolution function, we have modeled the line shape of the image-potential state. Most of the observed width of the image state comes from the instrumental resolution, but an upper limit of 0.10 eV can be obtained for the intrinsic width. This is consistent with two-photon photoemission data[33,34] which give an upper limit of 80 meV for the $n=1$ state in Ag(111). The lifetime broadening of the bulk states near the vacuum level is about 0.5 eV (Ref. 57) in noble metals. This broadening is mainly due to electron-hole pair creation in the bulk. Image-potential states overlap with bulk states much weaker than bulk states with each other since they are located significantly outside the surface (see Fig. 1). Both from the persistence of the image-potential states as surface resonance and from their narrow widths one can conclude that the coupling to the electronic states of the substrate crystal is rather weak in agreement with recent calculations.[57]

V. SURFACE CORRUGATION

The influence of the surface corrugation can be sought by comparing surfaces with various crystallographic orientations for the same material. The Cu(111), (100), and (110) surfaces (Fig. 7) exhibit increasing amount of surface corrugation. The binding energy of the $n=1$ image-potential state does not change dramatically. Actually, the observed trend in binding energy from 0.7 eV for Cu(111) to 0.64 eV for Cu(100) to 0.48 eV for Cu(110) (Ref. 58) is almost within the uncertainty given by the work-function determination. Surface corrugation is expected to give the opposite trend,[59] i.e., an increase in binding energy with increasing corrugation. The observed trend is qualitatively consistent with the predictions of a phase-shift analysis.[19,60,61] In this model (see below) the difference in binding energies for different surface orientations is not caused by the surface corrugation but by the different location of the bulk band gap at $k_{||}=0$ relative to the image-potential state. In order to separate the effects of surface corrugation and of location relative to the bulk band edges we have attempted to compare the metastable Au(100)1×1 surface with the Au(100)5×20 surface. The former is prepared by sputtering with oxygen, the latter by normal sputter annealing. Both surfaces have the same bulk band gap, but the 1×1 surface should have a larger corrugation than the 5×20 surface. It is difficult to obtain 1×1 surfaces with a reproducible work function, but within our accuracy we find no evidence for a change in binding energy due to surface corrugation.

VI. EFFECTIVE MASS

We have followed the dispersion of image-potential states with $k_{||}$ and find an effective mass larger than or equal to 1 but with large error bars. Other authors have reported effective mass values between 1.0 and 1.7 which are compiled in Table I. We note that the average deviation of the effective mass from unity is about 30% which is comparable with the deviation of the binding energy from the hydrogenic value. There have been various explanations for effective masses larger than unity[59,61–63] but the most straightforward arguments came from the phase-shift analysis.[61] In this model the dispersion of the bulk band edges influence the dispersion of the gap states. Image states near the top edge of the gap have $m^*/m_e>1$ and states near the bottom have $m^*/m_e<1$. Most image states that have been studied are located in the top half of the gap and therefore have $m^*/m_e>1$. Occupied surface states in the bottom half of the gap exhibit $m^*/m_e<1$.

VII. THEORETICAL MODELS

The observed binding energies E_B of image-potential states (Table I) match theoretical predictions by Echenique and Pendry[7,8] surprisingly well. They obtained $E_B=0.58$ eV for the $n=1$ state from an image potential that had been cut off near the surface (see Fig. 1). The calculated width of 0.32 eV (full width at half maximum) for the $n=1$ state is larger than our upper limit of 0.1 eV. This is due to the fact that the calculations were performed for high kinetic energies parallel to the surface where these states form resonances. A recent calculation for kinetic energy zero give a width of less than 0.1 eV.[57] These calculations suggest that we observe the $n=1$ image-potential state with only a small perturbation of the hydrogenic image potential which reduces the binding energy from 0.85 eV to the 0.5–0.8 eV observed. The sign of the energy shift[64] relative to the hydrogenic energy levels is plausible since the image potential is not infinitely deep for a real crystal but saturates at a value near the inner potential. Various workers[6–8,18,65] obtained qualitatively similar results by integrating the z-dependent Schrödinger equation with model potentials. A first-principles calculation[31] for Cu(100) comes to similar con-

clusions, giving the use of simple empirical potentials more credibility.

Instead of explicitly solving the Schrödinger equation one can use a scattering theory to derive binding energies of image-potential states.[2,7,8,19,26,60,61] In this picture the electron is reflected back and forth between the confining Coulomb potential barrier and the solid where it undergoes Bragg reflection. In order to obtain a stationary state the round-trip phase shift has to be a multiple of 2π. With a simple ansatz for the phase shifts at both boundaries, Hulbert *et al.*[19] and Smith[60,61] have given an elegant description of the trends that one expects for the binding energies and effective masses for a variety of surface states on different surfaces including image-potential states. Essentially, the image potential states shift upwards relative to their hydrogenic position the farther they are below the upper edge of the bulk band gap. As pointed out in Sec. V, we find our data to be consistent with these predictions although the experimental accuracy is not good enough to confirm this theory in a quantitative way. More precise two-photon photoemission experiments are under way[34] to this end.

Most theories of image potential states consider the z dependence of the potential only (z is perpendicular to the surface). Garcia and co-workers[59] present quite a different interpretation and stress the influence of the x,y dependence of the potential, i.e., the surface corrugation. They conclude that the interaction of the $n=1$ image-potential state with the periodic surface potential is so large that the state seen in the spectra actually corresponds to $n=2$. It is somewhat difficult to believe that the surface corrugation amounts to several eV for a state located about 8 Å outside the surface as required by this model. This model leaves several questions unanswered. If the periodic surface potential pulls the $n=2$ image state down almost to the position of the $n=1$ state, one would expect crystallographic effects, particularly, for the open crystal surfaces. The reduction in binding energy from Cu(111) to Cu(110), if real, would be opposite to the trend expected from the increase in corrugation. Recent experimental[33,34] and theoretical[31] work shows that the effect of corrugation is negligible and at least an order of magnitude smaller than predicted by Garcia *et al.*[59]

VIII. SUMMARY

In summary we find that the image potential induces electrons to be bound at the metal or semimetal surfaces with binding energies of 0.4—0.8 eV relative to the vacuum which are close to the energy of $\frac{1}{16}$ Ry=0.85 eV expected for a simple Coulombic potential. This phenomenon appears to be ubiquitous for metallic surfaces and does not depend strongly on details of the surface, such as crystallographic orientation, corrugation, reconstruction, and material. This shows that the simple Coulombic image potential dominates the energy balance and opens prospects for using this phenomenon to study an ideal two-dimension electron gas *in vacuo*.

ACKNOWLEDGMENTS

We acknowledge L. Ley for providing the Sb single crystal, M. Skibowski and W. Drube for providing the TiS_2 crystal, and K. Giesen for lending a Ag(111) crystal. We thank V. Dose, N. V. Smith, A. R. Williams, N. Garcia, and P. M. Echenique for stimulating discussions and A. Marx for his expert technical help.

[1]For a recent review on surface states, see F. J. Himpsel, Adv. Phys. **32**, 1 (1983).

[2]Electronic surface resonances are reviewed by E. G. McRae, Rev. Mod. Phys. **51**, 541 (1979).

[3]The two-dimensional electron gas at semiconductor interfaces and on liquid helium is reviewed by T. Ando, A. B. Fowler, and F. Stern, Rev. Mod. Phys. **54**, 437 (1982).

[4]M. W. Cole and M. H. Cohen, Phys. Rev. Lett. **23**, 1238 (1969); C. C. Grimes and G. Adams, *ibid.* **42**, 795 (1979).

[5]N. D. Lang and W. Kohn, Phys. Rev. B **7**, 3541 (1973); G. Kaindl, T.-C. Chiang, D. E. Eastman, and F. J. Himpsel, Phys. Rev. Lett. **45**, 1808 (1980).

[6]N. Garcia and J. Solana, Surf. Sci. **36**, 262 (1973).

[7]P. M. Echenique, Ph.D. thesis, University of Cambridge, 1976.

[8]P. M. Echenique and J. B. Pendry, J. Phys. C **11**, 2065 (1978).

[9]For $k_{||}$ values outside the first surface Brillouin zone the image-potential states can couple to propagating free-electron states via transfer of momentum equivalent to a reciprocal surface-lattice vector (surface umklapp). Thereby surface resonances are formed which show up in the elastic electron scattering cross section (for a review see Ref. 2). However, the mixing with continuum wave functions blurs the two-dimensional nature of these states and alternative explanations by simple interference effects have been given [see R. E. Dietz, E. G. McRae, and R. L. Campbell, Phys. Rev. Lett. **45**, 1280 (1980); J. C. LeBosse, J. Lopez, C. Gaubert, Y. Gautheir, and R. Bandoing, J. Phys. C **15**, 3425 (1982)].

[10]V. Dose, Prog. Surf. Sci. **13**, 225 (1983); H. Scheidt, Fortschr. Phys. **31**, 357 (1983); N. V. Smith, Vacuum **33**, 803 (1983); F. J. Himpsel and Th. Fauster, J. Vac. Sci. Technol. A **2**, 815 (1984); F. J. Himpsel, Comments Solid State Phys. (to be published).

[11]P. D. Johnson and N. V. Smith, Phys. Rev. B **27**, 2527 (1983).

[12]W. Altmann, V. Dose, A. Goldmann, U. Kolac, and J. Rogozik, Phys. Rev. B **29**, 3015 (1984).

[13]V. Dose, W. Altmann, A. Goldmann, U. Kolac, and J. Rogozik, Phys. Rev. Lett. **52**, 1919 (1984).

[14]D. Straub and F. J. Himpsel, Phys. Rev. Lett. **52**, 1922 (1984).

[15]D. A. Wesner, P. D. Johnson, and N. V. Smith, Phys. Rev. B **30**, 503 (1984).

[16]B. Reihl, K. H. Frank, and R. R. Schlitter, Phys. Rev. B **30**, 7328 (1984).

[17]D. P. Woodruff, S. L. Hulbert, P. D. Johnson, and N. V. Smith, Phys. Rev. B **31**, 4046 (1985).

[18]G. Thörner *et al.* (unpublished).

[19]S. L. Hulbert, P. D. Johnson, N. G. Stoffel, W. A. Royer, and N. V. Smith, Phys. Rev. B **31**, 6815 (1985).

[20]W. Altmann, M. Donath, V. Dose, and A. Goldmann, Solid

State Commun. 53, 209 (1985).
[21]B. Reihl and K. H. Frank, Phys. Rev. B 32, 8282 (1985).
[22]A. Goldmann, M. Donath, W. Altmann, and V. Dose, Phys. Rev. B 32, 837 (1985).
[23]See also D. Straub *et al.* (unpublished).
[24]A detailed account of image-potential states on transition-metal dichalcogenides will be given by W. Drube, I. Schäfer, and M. Skibowski (unpublished).
[25]S. L. Hulbert, P. D. Johnson, N. G. Stoffel, and N. V. Smith, Phys. Rev. B 32, 3451 (1985).
[26]A. Goldmann, V. Dose, and G. Borstel, Phys. Rev. B 32, 1971 (1985).
[27]W. Jacob *et al.* (unpublished).
[28]W. Altmann *et al.* (unpublished).
[29]J. Rogozik and V. Dose (unpublished).
[30]H. Scheidt, M. Glöbl, V. Dose, and J. Kirschner, Phys. Rev. Lett. 51, 1688 (1983).
[31]S. L. Hulbert, P. D. Johnson, M. Weinert, and R. F. Garrett (unpublished).
[32]Th. Fauster, F. J. Himpsel, J. J. Donelon, and A. Marx, Rev. Sci. Instrum. 54, 68 (1983); Th. Fauster, D. Straub, J. J. Donelon, D. Grimm, A. Marx, and F. J. Himpsel, Rev. Sci. Instrum. 56, 1212 (1985).
[33]K. Giesen, F. Hage, F. J. Himpsel, H. J. Riess, and W. Steinmann, Phys. Rev. Lett. 55, 300 (1985).
[34]K. Giesen, F. Hage, F. J. Himpsel, H. J. Riess, and W. Steinmann, Phys. Rev. B (to be published); K. Giesen *et al.* (unpublished).
[35]G. Binnig, K. H. Frank, H. Fuchs, N. Garcia, B. Reihl, H. Rohrer, F. Salvan, and A. R. Williams, Phys. Rev. Lett. 55, 991 (1985).
[36]R. S. Becker, J. A. Golovchenko, and B. S. Swartzentruber, Phys. Rev. Lett. 55, 987 (1985).
[37]See H. Eckardt, L. Fritsche, and J. Noffke, J. Phys. F 14, 97 (1984), and references given there.
[38]K. Besocke and S. Berger, Rev. Sci. Instrum. 47, 840 (1976).
[39]F. G. Allen and G. W. Gobeli, Phys. Rev. 127, 150 (1962).
[40]C. Sebenne, D. Bolmont, G. Guichar, and M. Balkanski, Phys. Rev. B 12, 3280 (1975).
[41]For E_{vac} on Au(111) we used the work function $\Phi=5.26$ eV from Ref. 43. Another reported value is $\Phi=5.3$ eV from F. Meier and D. Pescia, Phys. Rev. Lett. 47, 374 (1981).
[42]Th. Fauster, F. J. Himpsel, J. E. Fischer, and E. W. Plummer, Phys. Rev. Lett. 51, 430 (1983).
[43]G. V. Hansson and S. A. Flodström, Phys. Rev. B 18, 1572 (1978).
[44]M. Chelvayohan and C. H. B. Mee, J. Phys. C 15, 2305 (1982). In earlier work (Ref. 46) the work function was increased by sulfur contamination.
[45]B. Reihl and K. H. Frank (unpublished).
[46]A. W. Dweydari and C. H. B. Mee, Phys. Status Solidi A 17, 247 (1973); A 27, 223 (1975).
[47]J. Hölzl and F. K. Schulte, in *Solid Surface Physics,* Vol. 85 of *Springer Tracts in Modern Physics* (Springer, Berlin, 1979).
[48]P. O. Gartland, S. Berge, and B. J. Slagsvold, Phys. Norv. 7, 39 (1973).
[49]P. O. Gartland, Phys. Norv. 6, 201 (1972).
[50]W. Eib and S. F. Alvarado, Phys. Rev. Lett. 37, 444 (1976).
[51]F. J. Himpsel and D. E. Eastman, Phys. Rev. Lett. 41, 507 (1978).
[52]G. B. Baker, B. B. Johnson, and G. L. C. Maire, Surf. Sci. 24, 572 (1971).
[53]D. E. Eastman, Phys. Rev. B 2, 1 (1970).
[54]B. E. Nieuwenhuys and W. H. M. Sachtler, Surf. Sci. 34, 317 (1973).
[55]G. Pirug, G. Broden, and H. P. Bonzel, Surf. Sci. 94, 323 (1980).
[56]G. K. Binnig, H. Rohrer, Ch. Gerber, and E. Stoll, Surf. Sci. 144, 321 (1984).
[57]For the lifetime of bulk states see J. A. Knapp, F. J. Himpsel, and D. E. Eastman, Phys. Rev. B 19, 4952 (1979). For the lifetime of image states see P. M. Echenique, F. Flores, and F. Sols, Phys. Rev. Lett. 55, 2348 (1985).
[58]The image-potential state on Cu(110) is much weaker than on the other surfaces measured. A possible reason is the overlap with bulk states in the projected bulk band structure. [For the Cu bulk band structure along ΓKX see E. Dietz and F. J. Himpsel, Solid State Commun. 30, 235 (1979) and references therein.] Sample imperfections can be excluded because the crystal-induced surface state at about 2 eV above E_F for $k_{||}>0$ (see Ref. 21) was well resolved in off-normal measurements. An alternative explanation as a bulk density of states feature is not likely as this feature is sensitive to surface contamination.
[59]N. Garcia, B. Reihl, K. H. Frank, and A. R. Williams, Phys. Rev. Lett. 54, 591 (1985); an error by a factor of 4 in this calculation [32 instead of 128 in Eq. (3) in this paper] makes a quantitative comparison difficult. Therefore we discuss only the trend expected from this model.
[60]N. V. Smith, Appl. Surf. Sci. 22/23, 349 (1985).
[61]N. V. Smith, Phys. Rev. B 32, 3549 (1985).
[62]P. M. Echenique and J. B. Pendry (unpublished).
[63]G. Borstel and V. Dose (unpublished).
[64]A counteracting downwards shift of the levels is produced for a cut off image potential when the image plane moves away from the surface.
[65]M. Weinert, S. L. Hulbert, and P. D. Johnson, Phys. Rev. Lett. 55, 2055 (1985).